Copernicus Climate Change

Integration of Climate Data in the SAVi Roads Model

C3S_428h_IISD-EU: Sustainable Asset Valuation (SAVi): Demonstrating the Business Case for Climate-Resilient and Sustainable Infrastructure

Issued by: IISD-EU / Oshani Perera

Date: September 2020

Ref:

C3S_428h_IISD-EU_D428h.1.1 _202006_Integration of climate data in the SAVi model_v2

Official reference number service contract:

2019/C3S_428h_IISD-EU/SC1

Contributors

International Institute for Sustainable Development
Bechauf, Ronja
Casier, Liesbeth
Lago, Sergio
Perera, Oshani
Perrette, Mahé
Uzsoki, David
Wuennenberg, Laurin

KnowlEdge Srl
Bassi, Andrea M.
Pallaske, Georg

Table of Contents

1 About this Report

This report outlines the integration of authoritative Copernicus Climate Data from the Climate Data Store (CDS) into a Sustainable Asset Valuation (SAVi). It describes how several climate indicators obtained from the CDS were integrated into the SAVi Roads model and how the analysis performed by SAVi has improved as a result. In light of this integration, IISD is able to generate sophisticated SAVi-derived analyses on the costs of climate-related risks and climate-related externalities.

The integration of Copernicus Climate Data into other SAVi models for buildings, energy, irrigation, wastewater treatment infrastructure, and nature-based infrastructure can be found here.

This document presents:

- A summary of the literature review on the climate impact on roads, including the equations that link climate variables to the performance of roads.
- How the above information was used to select relevant indicators from the Copernicus database.
- How outputs of the CDS datasets are integrated into the SAVi System Dynamics (SD) Roads model.
- How simulation results can be affected by the use of this new and improved set of indicators.

This report is organized as follows.

Literature review

The literature review contains the following subsections for each of the climate variables discussed for road infrastructure:

- Subsection 1: An overview of the climate impacts on the asset (e.g., how precipitation affects roads).
- Subsection 2: A presentation of papers/reports that provide case studies that summarize the range of impacts estimated or observed (e.g., across countries).
- Subsection 3: A description of the methodology found in the literature for the calculation of climate impacts on the infrastructure asset.
- Subsection 4: A selection of CDS datasets required by the equations.

Integration of the Literature Review With the CDS Dataset

This section summarizes information on which datasets are being used from the Copernicus database and what additional processing was applied before integration into the SAVi Roads model for each asset. We first review the equations to determine their usefulness for the SAVi Road model. We assess what data requirements for each of the equations are available in the Copernicus database and create indicators for climate variables that are relevant for the equations selected. Finally, in certain cases, we create indicators in the CDS Toolbox for first-order impacts on infrastructure. Second- and third-order impacts will be estimated with SAVi, making use of additional equations included in the SD model.

Integration of Climate Indicators Into the SAVi Roads Model

This section explains how the CDS indicators are used in the SAVi SD model for road infrastructure. It includes an identification of specific performance indicators for each asset impacted by climate indicators (e.g., efficiency and cost).

Behavioural Impacts Resulting From the Integration of Climate Variables

This section discusses how climate variables affect asset performance in the SD model, providing early insights as to how the results of the SAVi analysis may change when equipping the model with more and better refined climate indicators (e.g., with the cost of infrastructure being higher due to increased maintenance, the economic viability of the infrastructure asset, presented as the Internal Rate of Return [IRR], will be lower than expected).

Simulation Results

The final section of this paper presents equations used and quantitative results emerging from the inclusion of climate indicators in the SAVi Roads model under various climate scenarios. This is the end product of the enhanced SAVi model, which is used to inform policy and investment decisions for infrastructure. Table 1 provides an overview of climate drivers, impacts, and relevant SAVi output indicators.

The CDS datasets are accessed via the CDS application programming interface (API), and additional processing and packaging for use in SAVi is done offline. Technical information about the offline code is found in Annex I. We also selected a subset of the most-used indicators and created an app in the CDS Toolbox with interactive visualization for demonstration purposes.

Table 1. Overview of variables and impacts implemented in the SAVi Roads model

SAVi module	Implemented impact	Main climate drivers	Affected output indicators
Roads	Stormwater runoff from roads	• Precipitation	• Stormwater management cost

SAVi module	Implemented impact	Main climate drivers	Affected output indicators
	Effect of precipitation on road lifetime	• Precipitation	• Depreciation of roads • Cost of road construction and maintenance • Road-related energy use • Energy-related emissions • Social cost of carbon
	Weather effects on accident rates	• Precipitation • Temperature	• Number of accidents • Economic cost of accidents

2 Roads

2.1 Literature review

2.1.1 Infrastructure impacts

Roads are impacted differently by climate variables, depending on how they are built and the materials used. Precipitation, snow, high temperatures imply higher costs of maintenance (operating costs). If maintenance is not timely, the reduced quality of roads can lead to the emergence of structural problems and increase the probability of accidents.

2.1.1.1 Precipitation

- **Climate impact**

High amounts of precipitation can damage roads, depending on surface permeability and materials used. Surface runoff is an indicator commonly used to determine the extent to which a road is exposed to damage due to precipitation.

- **Summary of results**

Runoff holding capacity for an Interlocking Block Pavement with Gravel is of 136mm per rainfall depth and for Porous Concrete Pavement, the normalized volume reduction was $2.81 \times 10^{-3} \pm 0.67 \times 10^{-3}$ $m^3/m^2/mm$.
There is also a study that concluded that for every 10mm of monthly rainfall, rut depth would increase by 3mm.

- **Results**

Chinowsky et al. (2013) estimated that for the maintenance of roads in the US, rut depth over a road's lifecycle increases by approximately 3mm with every 10 cm increase in mean monthly rainfall. This implies higher road maintenance with heavy rainfall.

When considering runoff efficiency, Alam et al. (2019) showed that IBPG (Interlocking Block Pavement with Gravel) was capable of holding runoff from rainfall depths up to 136 mm prior to flooding.
PCP (Porous Concrete Pavement) was the most satisfactory in reducing surface runoff (NVR (Normalized Volume Reduction): $2.81 \times 10^{-3} \pm 0.67 \times 10^{-3}$ $m^3/m^2/mm$), which was significantly higher than the traditional pavement.

- **Methodology**

2.1.1.2 Runoff efficiency

Alam et al. (2019) examined the hydrologic and environmental performance of three types of permeable pavement designs: Porous Concrete Pavement (PCP), Permeable Interlocking Concrete (PICP), and Interlocking Block Pavement with Gravel (IBPG) in the semi-arid South Texas.

Equations (1)–(5) show the approach used to calculate the total inflow volume into the pavement surface, % peak flow reduction, total outflow volume at the pavement's outfall, total volume stored into pavements, and Normalized Volume Reductions (NVR) from monitored permeable and traditional pavements.

1. Total inflow volume:

$$V_i = R\left(A_p + C_1A_1 + C_2A_2 + C_3A_3 \ldots\ldots\right) \quad (1)$$

V_i = Total Inflow Volume onto Pavement Surface (m^3)
R = Rainfall Depth (mm)
A_p = Permeable Pavement Area (m^2)
A1, A2, A3 = Areas from Surrounding Drainage Sources (m^2)
C1, C2, C3 = Runoff Coefficients of Surrounding Drainage Sources

2. The % peak flow reduction for all monitored permeable pavements:

$$\%\ Peak\ Flow\ Reduction = \left(\frac{TP_{PF} - PP_{PF}}{TP_{PF}}\right) \times 100 \quad (2)$$

TP_{PF} = Normalized peak flow rate at the outfall of traditional pavement (m^3/s)
PP_{PF} = Normalized peak flow rate at the outfall of alternative pavement (m^3/s)

3. Volume of runoff:

$$V_o = q_0 \times t \quad (3)$$

V_o = Total Runoff Volume (m^3)
q_0 = outflow rate (m^3/s)
t = Flow Duration (s)

4. Storage volume:

$$S = V_i\ (1) - V_o\ (3)$$

5. Normalized Volume reduction (NVR):

$$\left(\frac{m^3}{m^2 \cdot mm}\right) = \frac{V_i - V_o}{A_p \times R} \quad (5)$$

Considerations for integration in the CDS toolbox

ERA5 hourly data on single levels from 1979 to present

2.1.1.3 Flood risk

See section on flood risk for buildings, proposing the creation of a non-linear function based on a report by Nemry and Demirel (2012).

2.1.1.4 Temperature and freeze-thaw

According to Chinowsky et al. (2013) freeze–thaw effects are worst in moderate freeze areas. When a former moderate freeze area transitions to a low freeze area due to higher temperatures, this reduces rutting of the road and therefore maintenance costs. Increased temperatures also cause some areas to change from high freeze to moderate freeze, which increases rutting and maintenance costs. Moderate freeze areas are defined to have 50–400 freeze days per year, high freeze areas have more than 400 freeze days per year. Freezing degree-days are usually calculated as a sum of average daily degrees below freezing for a specified time period (National Snow & Ice Data Center, n.d.). Rut depths in moderate freeze areas and high freeze areas are approximately 3.25 and 2.75 mm higher, respectively, than in no-freeze zones (Jackson & Puccinelli, 2006).

2.1.1.5 Temperature

As presented in Chinowsky et al. (2013), higher temperatures imply higher stress for paved roads, as the asphalt becomes more susceptible to cracking. Cracking can be avoided by using a different binder in the surface asphalt.

2.1.2 Maintenance

2.1.2.1 Precipitation

- **Summary of results**

Regarding specific changes in precipitation, we have that maintenance costs increase by 0.8% with every 1% increase in maximum monthly precipitation.
Degradation is of 5.625 points per millimeter of rutting is related to precipitation per year and 7.83 points per millimeter of rutting related to freeze–thaw.

- **Results**

Method 1

Chinowsky et al. (2013) propose an equation based on a study conducted on the US road network, taking rutting (or rut depth) as a measure of road depreciation. The approach assumes that higher rutting leads to shorter maintenance intervals, and hence overall maintenance costs. For paved roads, they included three climate-related effects on roads: (1) rutting from precipitation, (2) rutting caused by freeze–thaw cycles, (3) cracking during periods of high temperatures. For unpaved roads, only the erosion from precipitation was calculated.

There are different estimates of the rutting occurring over a road's lifecycle: (N.D. Lea International, 1995) estimates 8 mm of rutting over a road's lifecycle, while (Lavin, 2003) estimates 5.75 mm of rutting. Based on these values, degradation of 5.625 points per millimeter of rutting is estimated related to precipitation and 7.83 points per millimeter of rutting related to freeze–thaw (Chinowsky, Price, & Neumann, 2013)**.**

Quote from article:
"Measurements of the degree of rutting occurring over a road's lifecycle vary across the identified studies. N.D. Lea International (1995) estimates 8 mm of rutting over a road's lifecycle, while U.S. DOT (2006) estimates 5.75 mm of rutting.
To estimate RC, we draw from prior studies examining the rutting associated with precipitation and freeze– thaw, and subsequently assess the changes in pavement condition index associated with these rutting impacts. N.D. Lea International (1995) indicates that rut depth over a road's lifecycle increases by approximately 3 mm with every 10 cm increase in mean monthly rainfall. In addition, U.S. DOT (2006) shows that rut depths in moderate freeze areas (50–400 freeze days per year) and high freeze areas (more than 400 freeze days per year) are approximately 3.25 and 2.75 mm higher, respectively, than in no-freeze zones."

Equation: Based on the above, the equation proposed is the following

Impact of precipitation on road maintenance =
1 + (Precipitation - Mean precipitation)/100 * 0.375

Method 2 (Chinowsky, et al., 2011)

The approach is based on the cost of preventing a reduction in lifespan that may result from changes in climate-related stress. Chinowsky et al. (2011) assume that a reduction in lifespan is equal to the percent change in climate stress (scaled for the stressor's effect on maintenance costs).

According to (Miradi, 2004) maintenance for paved roads that is precipitation-related accounts for 4% of maintenance costs and temperature-related maintenance accounts for 36% of costs.

The costs of avoiding a reduction in lifespan is calculated by the product of (1) the potential percent reduction in lifespan and (2) the base construction costs of the asset. This means that a 10% potential reduction in lifespan causes an estimated increase in maintenance costs of 10% of the construction costs (Chinowsky, et al., 2011).

Unpaved roads are strongly influenced by precipitation. According to (Ramos-Scharron & MacDonald, 2007) 80% of unpaved road degradation can be attributed to precipitation, and the remaining 20% to traffic rates and other factors. Given this 80% attribution to precipitation, maintenance costs increase by 0.8% with every 1% increase in the maximum of the maximum monthly precipitation values projected for any given year (Chinowsky, et al., 2011).

Considerations for integration in the CDS toolbox

ERA5 monthly averaged data on single levels from 1979 to present

2.1.2.2 Temperature

- **Summary of results**

In present value terms, costs emerging from higher temperatures range from 140$ per mile under Global Action scenario, which means 1.2% increase in costs, to 475$ per mile under BAU scenario that means an increase of costs of 2.7%. Annual adaptation costs would be in the range of $3000 to $3600 for 2006 through 2080 per lane-mile.

- **Results**

Higher temperatures imply higher stress for roads materials that can melt, crack and be affected by the daily flow of road traffic. Higher temperatures can also change the freeze-thaw effects. Precipitation influences a roads' maintenance costs, especially in case of unpaved roads.

In the US, Chinowsky et al. (2013) estimated that overall, climate change, if unchecked, will increase the annual costs of keeping paved and unpaved roads in service by $785 million in present value terms by 2050. When not discounted, this figure increases to $2.8 billion. They estimate annual adaptation costs ranging from $140 per lane mile in 2025 under the Global Action scenario and $475 per lane mile in 2075 under the business as usual scenario. This suggests a 1.2% increase in costs in 2075 under Global Action scenario and a 2.7% increase under the business as usual case.

Chinowsky et al. (2013) compared their results with a study from (Larsen, et al., 2008) about adaptation costs for roads in Alaska. Chinowsky et al. (2013) based the comparison on converting the Larsen et al. (2008) estimates to year 2010 dollars and expressing these estimates on a cost-per-lane-mile basis, assuming two lanes per road. Thus, the annual adaptation costs per lane mile are estimated to be $3000 to $3600 for 2006 through 2080. Larsen et al. (2008) results imply a 5.6–5.8% increase in road construction and maintenance costs during the 2006–2080 period. The higher estimates in Larsen et al. (2008) can be attributed to stronger climate changes in Alaska and the additional consideration of costs related to flooding and the melting of permafrost.

- **Methodology**

Method 1 (Chinowsky, Price, & Neumann, 2013)

Costs are estimated under a baseline scenario in which annual mean global temperature increases by 1.5 degree Celsius in 2050 relative to the historical average, and a mitigation scenario under which this increase in mean temperature is limited to 1.0 degree Celsius.

To assess the cost of adapting roadways to changes in temperature, they examine the implications of climate change for the design specifications of asphalt pavements. In areas where maximum temperatures increase due to climate change, asphalt pavements will become susceptible to increased cracking.

1. The cost (savings) of adapting paved roads to higher (lower) temperatures is estimated as the incremental cost of repaving with a higher (lower) grade binder:

As an initial step in this process, the daily pavement temperature is estimated for each 0.58 by 0.58 grid cell under current climate and under each climate change scenario based on a book written by Lavin (2003)

$$T_P = 0.9545(T_A - 0.00618L^2 + 0.2289L + 42.2) - 17.78 \qquad (5)$$

where T_P is the pavement temperature (°C), T_A is the air temperature (°C) and L is the latitude.

2. 7 day pavement temperature is used to determine the level of adaptation of asphalt binder. We can use an average function and average the last 7 days of this variable to determine the extra cost of maintenance.

Effect of heat on road maintenance costs (binder, based on variable above):

Additional cost for road maintenance = f(Tp Max 7 day)

The indicated cost of binder use is illustrated in the "additional data" tab. based on 7 day pavement temperature. This applies to construction as well, if we are assuming that binders in planned roads will be already updated.

Considerations for integration in the CDS toolbox

Air temperature (K) - ERA5-Land hourly data from 1981 to present

Method 2 (Zhao, Shen, & Ma, 2018)

Temperature adaptability of asphalt pavements is very important, due to their potential influence on pavement structure design, particularly in areas that experience significant temperature differences.

To calculate pavement radiation and convection, the precondition is to identify the pavement surface temperature, and the research of Tang (2012)was referred to:

$$T_{sur} = 1.0852\,T_{air} - 0.0684\,h + 4.29, \qquad (6)$$

where T_{sur} (°C) is the pavement surface temperature, T_{air} (°C) is the air temperature, and h (m) is the pavement depth.

Hourly surface temperature requires an assumption on pavement depth.

Considerations for integration in the CDS toolbox

Air temperature (K) - ERA5-Land hourly data from 1981 to present

2.1.3 Accidents

Rainfall and temperature can impact accidents. Literature shows that accidents are higher with higher rainfall. Also, fatal accidents seem to be higher when temperatures are high, while fatality is the lowest when the weather is bad or icy roads are found. This points to the important of the driver (attention and skills) in addition to the quality of the road.

2.1.3.1 Temperatures / Precipitation

- **Climate impact**

Weather conditions are considered to be a factor that affects the number of road accidents and casualties significantly, with different effects according to the type of road (motorways, rural roads or urban roads). Moreover, as the weather also affects mobility, it is to be expected that the effects of weather on the number of injury accidents and casualties are partly due to the changes in mobility occurring at the same time. (Bergel-Hayat, Debbarh, Antoniou, & Yannis, 2013)

- **Summary of results**

When rainfall increases by 100mm per month, the probability of a road accident increases by 0.2-0-3%. For monthly temperature, an increase of 1˚C is equal to an increase of road accident probability of 1-2%. Finally, 1 day of frost more per month is equal to an increase of probability of 0.3-0.6% of road accident.

- **Results**

A study regrouping datasets for France, the Netherlands and the Athens region has been analyzed to highlight the link between weather conditions and road accident risk at an aggregate level and on a monthly basis (Bergel-Hayat, Debbarh, Antoniou, & Yannis, 2013).
Results on a national level are that 100 mm of additional rainfall during a month increases the number of injury accidents in that month by 0.2–0.3% (NED/FR); 1°C of additional average temperature during a month increases the number of injury accidents in that month by 1–2% and

finally that 1 additional day of frost during a month decreases the number of injury accidents in that month by 0.3–0.6%.

- **Methodology**

Injury accident multiplier = 1 + (RF - mean RF)/100 * 0.002 + IF THEN ELSE (Time > March: AND: Time < October, (ST - mean ST) * 0.02, 0) + IF THEN ELSE (Time > October: AND: Time < March, (WT - mean WT) * 0.006,0)) + (DF - mean DF) * 0.006

RF = monthly precipitation
Mean RF = mean precipitation (for each month)
ST = monthly summer temperature (March - September)
Mean ST = mean temperature for summer months (by month)
WT = monthly winter temperature (October - February)
Mean WT = mean temperature for winter months (by month)
DF = Days of frost (per month)
Mean DF = mean days of frost per month

The data used is based on the general conclusions for national highway networks. The numbers used relate to the Netherlands and France, but geographical factors matter. It was for example also found that ice causes more accidents, but less deadly accidents due to driver anticipation.

Considerations for integration in the CDS toolbox

ERA5-Land monthly averaged data from 1981 to present
ERA5 monthly averaged data on single levels from 1979 to present

2.2 Integration of literature review with the CDS datasets

See section 1.2 fora general introduction.

Datasets:

- ERA5 monthly data on single level
- CMIP5 monthly data on single level
- ERA5 hourly data on single level

Indicators created:

- **Monthly 2-m temperature**
  - Units: degrees Celsius
  - Frequency: monthly
  - ERA5 variable: “2 m temperature”
  - CMIP5 variable: “2 m temperature“
  - Note: original units in Kelvin
- **Monthly precipitation**:

- Units: mm per month
- ERA5 variable: “Mean total precipitation rate”
- CMIP5 variable: “Mean precipitation flux“
- Note : original units in mm/s

- **Monthly evaporation**
  - Units: mm per month
  - ERA5 variable: “Mean evaporation rate”
  - Note: original units in mm/s
- **Monthly surface runoff**
  - Units: mm per month
  - ERA5 variable: “Mean surface runoff rate”
  - Note: original units in mm/s

2.3 Integration of climate indicators into the SAVi roads model

CDS climate indicators developed for the roads sector include climate impacts on road lifetime, stormwater management and road safety. Figure 49 presents the CLD for the SAVi Road asset model; CDS climate indicators are highlighted in pink.

Figure 1 Causal Loop Diagram for the roads sector - CDS variables included

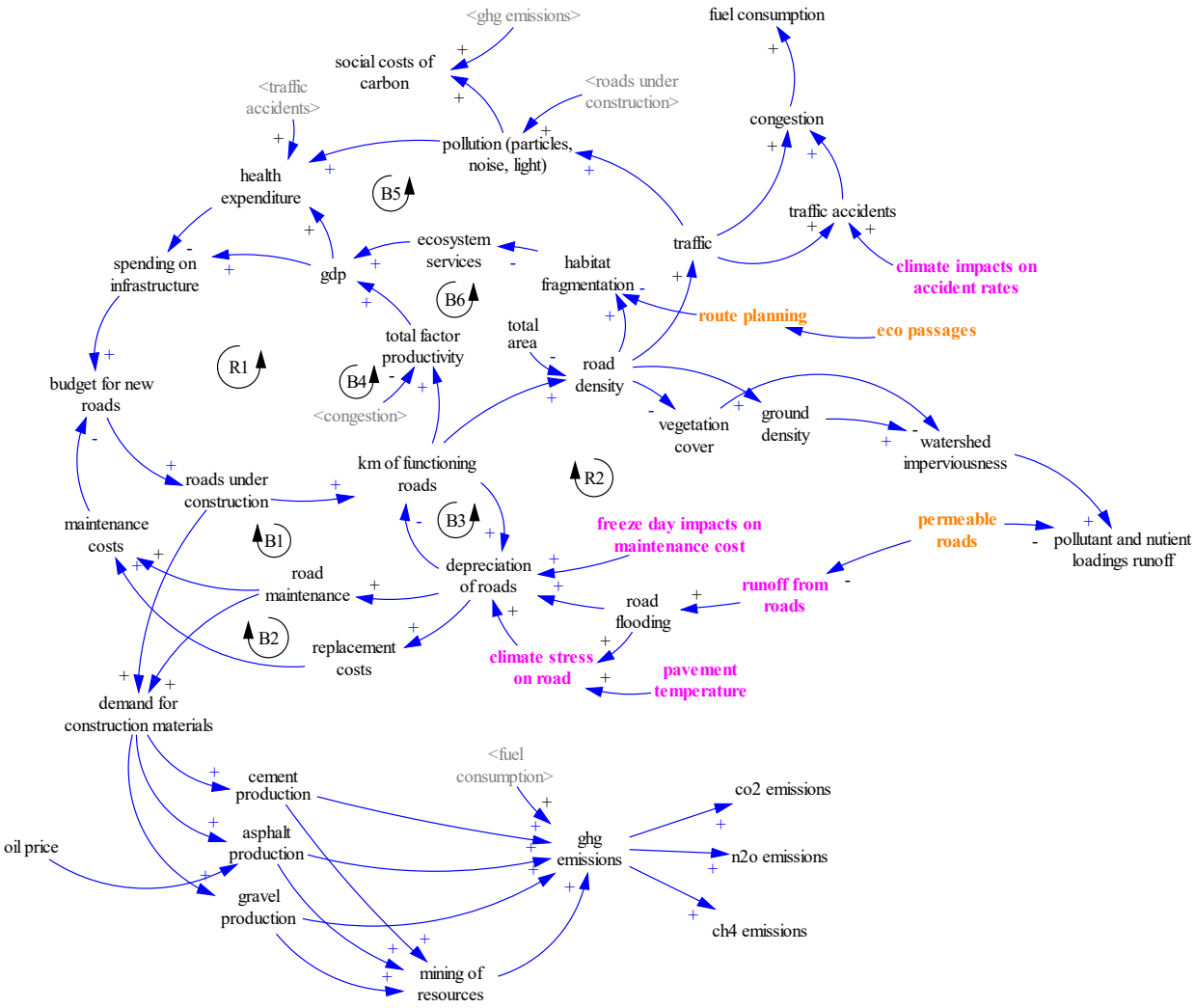

Weather impacts on road lifetime, increasing depreciation of the road surface as a consequence of temperature extremes (both increasing temperatures and more frequent freezing days) and precipitation. CDS indicators developed for the model include the impact of precipitation on pavement lifetime as well as the impact of air temperature on pavement integrity. Increases in mean precipitation causes the road surface to depreciate at a higher rate. Similarly, heat stress impacts are captured using pavement temperature. In both cases, CDS impacts lead to a reduced operational lifetime of roads, additional maintenance required and, as a consequence, material use.

The stormwater indicator developed in the CDS toolbox provides information about the water runoff from road surfaces during precipitation events. Stormwater, if not properly managed, can cause traffic disruptions and a multitude of environmental impacts due to the pollutants that are carried off the road into the environment (creating a direct connection with stormwater management).

The CDS toolbox indicator for road safety refers to changes in accident rates based on weather conditions. Variables such as precipitation, temperature, icy days and sunshine hours have an impact on traffic patterns and accidents. Depending on the change of climate variables, accident rates will increase or decrease.

2.4 Behavioral impacts resulting from the integration of climate variables

Climate impacts on the operational lifetime of roads and pavement layers cause higher maintenance frequency and hence increases material use and maintenance costs (both due to higher temperature and freezing days). Changes in maintenance frequency further affect energy use for road maintenance and road-related GHG. The use of CDS data allows for a more precise and location-specific assessment of road performance, with a more reliable estimate of maintenance costs.

The CDS indicator related to pavement temperature affects road construction and maintenance related costs by affecting the type of binder required. The indicator provides information about changes in cost related to the requirement of using a specific binder.

Obtaining stormwater quantities directly from the CDS toolbox improves capturing seasonal changes in stormwater loads and stormwater management related costs. This improves the modelling of mitigation measures, required stormwater management capacity and related investment and maintenance costs.

Climate impacts on accidents affect the number of accidents per million vehicle kilometers travelled, causing changes in the total number of accidents and related health cost. This indicator contributes to improving the modeling of seasonal accident patterns, and informs decisions about the type pavement used (e.g. depending on desired permeability) to avoid societal costs. The information obtained can support the road management and design process, depending on the forecasted magnitude of climate impacts on accidents.

2.5 Simulation results

Three impacts were integrated into the SAVi Roads model, based on climate data obtained from the CDS data base: (1) precipitation effect on road lifetime, (2) weather effect on injury accidents, and (3) precipitation based road runoff.

2.5.1 Impact of precipitation on road lifetime

According to the literature (N.D. Lea International, 1995; Lavin, 2003), precipitation is responsible for approximately 37.5% of road depreciation, also expressed as rutting depth. The equation used for operationalizing the impacts of precipitation on road maintenance is

*Impact of precipitation on road maintenance = 1 + (Precipitation - Mean precipitation)/100 * 0.375*

Simulation results comparing the no climate simulation to the simulation with CDS indicators are presented in Figure 50. On the left, the simulation results for roads lifetime are illustrated while the graph on the right provides information about the replacement rate of roads, both comparing the no climate scenario (red) to the CDS integration (blue).

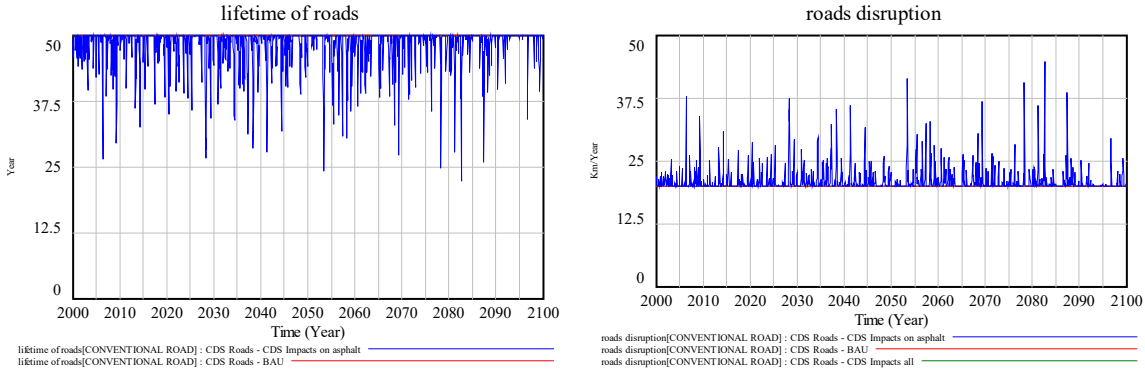

Figure 2: Impact of precipitation on roads lifetime (left) and road disruption rate (right) in the BAU and CDS scenario

Reductions in roads lifetime are simulated on a monthly level, leading to a change in road disruption and consequently in required road works. The monthly changes in lifetime and road disruption provide a more nuanced perspective on the impacts of severe events and the seasons during which the highest impacts occur. In the no climate scenario (red), the roads lifetime is forecasted to be 50 years constant.

Over a 80 year period (2020-2100), the forecasted additional disruption for 1,000 km of road resulting from the integration of CDS climate data is 5.45%, or 87.26km. In the no climate scenario, the cumulative reconstruction of roads is 1,601.67 km over 80 years, while the forecasted cumulative disruption of roads in the CDS scenario is 1,688.9 km.

2.5.2 Impact of weather on accidents

Weather affects driving behavior and the number of injury accidents occurring during specific seasons of the year. For example, when the roads are icy, studies indicate a reduction in injury accidents resulting from more careful driving behavior. The same applies for higher temperatures, which have been found to cause more aggressive driving behavior.

Bergel-Hayal et al (2013) describe the relationship between climate variables (precipitation and temperature) and accident frequency. A 100mm increase in monthly precipitation yields a 0.2-0.3% increase in accidents fractions, and 1°C increase in mean monthly temperature increases accidents by 1-2% (Bergel-Hayat, Debbarh, Antoniou, & Yannis, 2013). The equation used for estimating the impacts of weather on accidents is described below.

*Injury accident multiplier = 1 + (RF - mean RF)/100 * 0.002 + IF THEN ELSE (Time > March: AND: Time < October, (ST - mean ST) * 0.02, 0) + IF THEN ELSE (Time > October: AND: Time < March, (WT - mean WT) * 0.006,0)) + (DF - mean DF) * 0.006*

RF = monthly precipitation
Mean RF = mean precipitation (for each month)
ST = monthly summer temperature (March - September)
Mean ST = mean temperature for summer months (by month)
WT = monthly winter temperature (October - February)
Mean WT = mean temperature for winter months (by month)
DF = Days of frost (per month)
Mean DF = mean days of frost per month

The difference in injury accidents between the BAU (red line) and including CDS climate impacts (blue line) is presented in Figure 51.

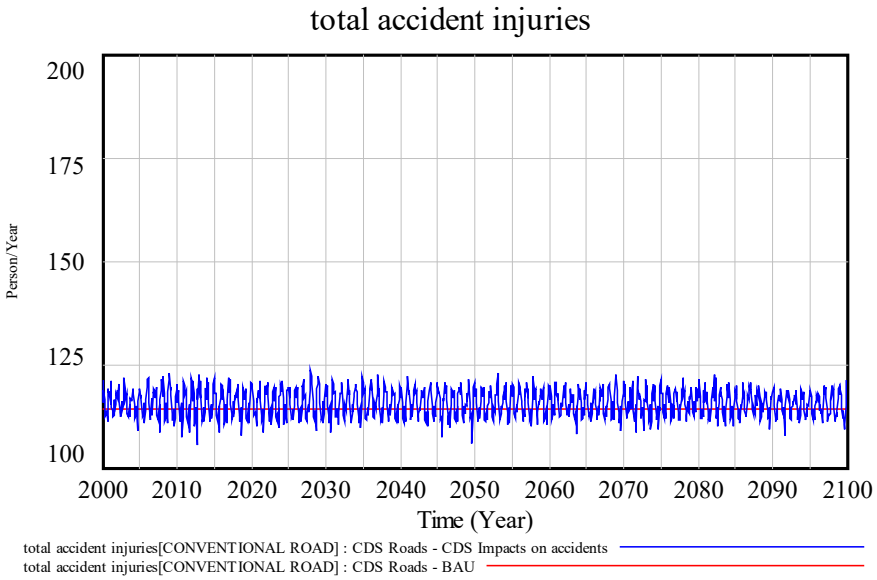

Figure 3: Injury accidents in the BAU and the CDS climate scenario

Compared to the no climate scenario, we observe an increase of injury accidents during summer times, and a decline in injury accidents during the winter season. This change in accidents leads to a change in physical and economic damages resulting from traffic accidents throughout the year (and the whole simulation).

Between 2020 and 2100, the forecasted number of injury accidents is 1.2%, or 1,324 accidents higher in the CDS scenario compared to the no climate scenario. On average, this corresponds to approximately 16.5 additional traffic accidents per year over a period of 80 years. As a consequence of more injury accidents, injury accident related damages will be 1.2% higher as well.

2.5.3 Runoff and stormwater management

Roads runoff and resulting stormwater loads pose a challenge to asset managers, especially in urban environments. The need to mitigate stormwater loads to maintain traffic and prevent flood damages requires an accurate forecast of stormwater loads from roads.

Stormwater runoff from roads depends on the total amount of rainfall and the runoff coefficient of roads, whereby the latter indicates their permeability and capacity to store water. The equation for estimating stormwater runoff from roads is described as

*Runoff from roads = Monthly precipitation * Runoff coefficient for roads * Conversion from mm per hectare to liters*

The change in roads runoff and resulting stormwater in the CDS integration scenario is presented in Figure 52. The results show a significant difference between the initial setup of the SAVi model and the results obtained from the CDS integration.

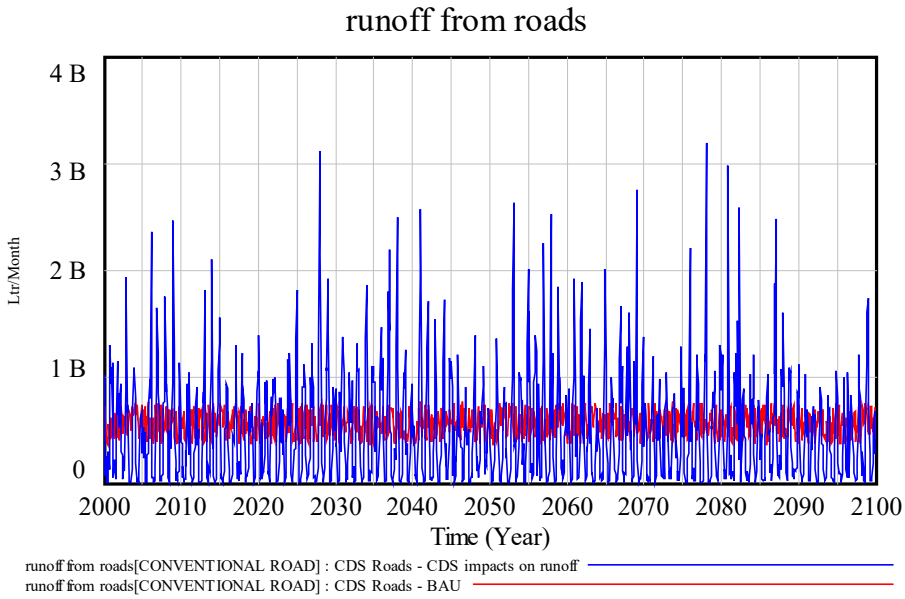

Figure 4: Runoff from roads CDS scenario compared to the BAU sceario

While runoff is relatively constant in the no climate scenario, the CDS integration shows differences both in terms of seasonality and magnitude of stormwater loads. In terms of the magnitude of impacts, the maximum monthly stormwater loads forecasted in the no climate scenario is 758.63 million liters and the cumulative amount of stormwater between 2020 and 2100 is 466.43 billion liters for 1,000m km of road. In comparison, the maximum monthly stormwater load resulting from the integration of CDS climate variables is 3,182.3 million liters and the cumulative amount over an 80 year period is 534.48 billion liters. The highest difference in monthly maximum values is 319%, and the difference in observed minimum runoff during the dry period is 99.92%, meaning that the simulation indicates 0.08% of BAU runoff during the dry period.

The above indicates that the previous formulation used for estimating stormwater runoff from roads underestimated the total maximum loads and overestimated stormwater loads during periods with low precipitation. In summary, the results indicate that the BAU simulation underestimated total cumulative runoff by around 68.05 billion liters over 80 years.

2.5.4 Economic impacts resulting from the integration of CDS climate variables

The physical impacts resulting from the integration of CDS based climate impacts leads to a change in road management costs and related externalities. The integrated Cost Benefit Analysis (CBA) presented in Table 20 provides an overview of the cumulative costs for each scenario. The results presented provide cumulative figures for the period 2020 to 2100 in USD million.

Impacts related to asphalt indicate an increase in capital expenditure for road construction and the cost of road maintenance. Over an 80 year period, the additional cost of road construction totals USD 9.4 million, while additional maintenance costs are projected to be in the range of 87,000 USD. The additional labor income generated from employment related to road construction and maintenance is forecasted at USD 25.8 million between 2020 and 2100. On a system level, these impacts yield positive results (net positive impacts of USD 8 million) if the labor income generated by the additional construction and maintenance is considered.

The integration of weather into the equation for injury accidents indicates that the additional economic cost of traffic accidents is 21.9 million USD between 2020 and 2100, or 272,500 USD per year on average.

The most significant difference in economic cost results from the updated formulation for stormwater runoff. Based on the differences in stormwater loads described above, the additional cost of stormwater management is projected at 2.06 billion USD over 80 years. This is equivalent to an additional annual cost of USD 25.58 million on average.

Considering all impacts at the same time (scenario 4 in CBA), the total difference between the no climate scenario and the scenario considering CDS climate impacts totals USD 2.08 billion between 2020 and 2100, out of which the largest share comes from stormwater management. This analysis assumes that all stormwater is conveyed and treated, which is not necessarily a realistic assumption.

Indicator	Unit	0. No Climate	1. Impacts on asphalt	*1. vs no climate*	2. Impacts on accidents	*2. vs no climate*	3. Impacts on runoff
Investment and cost							
Capital cost	mln USD	185.0	194.4	*9.4*	185.0	*0.0*	185.0
O&M costs	mln USD	34.9	35.0	*0.087*	34.9	*0.000*	34.9
Total cost	mln USD	219.9	229.4	*9.5*	219.9	*0.0*	219.9
Externalities							
(1) Positive							
Labor income	mln USD	1,348.8	1,374.6	*25.8*	1,348.8	*0.0*	1,348.8
(2) Negative							
Cost of traffic accidents	mln USD	759.5	761.4	*1.9*	781.5	*21.9*	759.5
Social cost of carbon	mln USD	14.7	14.7	*0.0*	14.7	*0.0*	14.7
Stormwater management cost	mln USD	2,423.6	2,429.9	*6.3*	2,423.6	*0.0*	4,481.1
Cost of nitrogen removal	mln USD	1.6	1.6	*0.0*	1.6	*0.0*	1.6
Net sum of externalities (1) - (2)	mln USD	1,850.5	1,833.0	*-17.5*	1,872.5	*21.9*	3,908.0
Total integrated cost	**mln USD**	**2,070.4**	**2,062.4**	***-8.0***	**2,092.4**	***21.9***	**4,127.9**

Table 2: Integrated Cost Benefit Analysis assessing the differences between the BAU and the CDS integration

3 Bibliography

Acclimatise. (2009). *Building Business Resilience to Inevitable Climate Change. Carbon Disclosure Project Report. Global Electric Utilities.* Oxford.

Adeh, E. H., Good, S. P., Calaf, M., & Higgins, C. W. (2019). Solar PV Power Potential is Greatest Over Croplands. *Scientific reports, vol(9), no(1)*, pp. 1-6.

Ahsan, S., Rahman, M. A., Kaneco, S., Katsumata, H., Suzuki, T., & Ohta, K. (2005). Effect of temperature on wastewater treatment with natural and waste materials. *Clean Technologies and Environmental Policy, 7(3)*, 198-202.

Akbari, H. (2005). *Energy saving potentials and air quality benefits of urban heat island mitigation.* Récupéré sur OSTI.org: https://www.osti.gov/biblio/860475/

Akbari, H., Davis, S., Dorsano, S., Huang, J., & Winnett, S. (1992). *Cooling our communities: A guidebook on tree planting and light-colored surfacing.* Washington, DC (United States): Lawrence Berkeley Lab.; Environmental Protection Agency.

Alam, T., Mahmoud, A., Jones, K. D., Bezares-Cruz, J. C., & Guerrero, J. (2019). A Comparison of Three Types of Permeable Pavements for Urban Runoff Mitigation in the Semi-Arid South Texas, USA. *MDPI - Water, 11(10)*.

Allen, R. G., Pereira, L. S., Raes, D., & Smith, M. (2006). *FAO Irrigation and Drainage Paper - Crop Evapotranspiration.* FAO.

Allos, M. (2016, Juin). *Potential Damage Caused by Direct Lightning Strikes*. Récupéré sur Sollatek: https://www.sollatek.com/potential-damage-caused-direct-lightning-strikes/

American Society of Landscape Architects. (2003). *Chicago City Hall Green Roof*. Récupéré sur asla.org: http://www.asla.org/meetings/awards/awds02/chicagocityhall.html

Asian Development Bank. (2012). *Adaptation to Climate Change - The Case of a Combined Cycle Power Plant.* Philippines.

Attia, S. I. (2015). The influence of condenser cooling water temperature on the thermal efficiency of a nuclear power plant. *Annals of Nuclear Energy*, 371-378.

Bartos, M., Chester, M., Johnson, N., Gorman, B., Eisenberg, D., Linkov, I., & Bates, M. (2016). Impacts of rising air temperatures on electric transmission ampacity and peak electricity load in the United States. *Environmental Research Letters, 11(11), 1*.

Basha, M., Shaahid, S. M., & Al-Hadhrami, L. (2011). Impact of fuels on performance and efficiency of gas turbine power plants. *2nd International Conference on Advances in Energy Engineering*, (pp. 558-565). Bangkok.

Bassi, A. M., Pallaske, G., Wuennenberg, L., Graces, L., & Silber, L. (2019, March). *Sustainable Asset Valuation Tool: Natural Infrastructure.* Récupéré sur International Institute for Sustainable Development : https://www.iisd.org/sites/default/files/publications/sustainable-asset-valuation-tool-natural-infrastructure.pdf

Bengtson, H. (2020). *The Rational Method for Estimation of Design Surface Runoff Rate for Storm Water Control*. Récupéré sur brighthubengineering.com: https://www.brighthubengineering.com/hydraulics-civil-engineering/60842-the-rational-method-for-calculation-of-peak-storm-water-runoff-rate/

Bergel-Hayat, R., Debbarh, M., Antoniou, C., & Yannis, G. (2013). Explaining the road accident risk: weather effects. *Accident Analysis & Prevention, 60*, 456-465.

Berghage, R. D., Beattie, D., Jarrett, A. R., Thuring, C., Razaei, F., & O'Connor, T. P. (2009). *Green Roofs For Stormwater Runoff Control.* Cincinnati: EPA.

Bhatt, S., & Rajkumar, N. (2015). Effect of moisture in coal on station heat rate and fuel cost for Indian thermal power plants. *Power Research, 11(4)*, 773-786.

Bhattacharya, C., & Sengupta, B. (2016). Effect of ambient air temperature on the performance of regenerative air preheater of pulverised coal fired boilers. *Int. J. Energy Technology and Policy, Vol. 12, No. 2*, pp. 136–153.

Biswas, B. (2014). Construction and Evaluation of Rainwater Harvesting System for Domestic Use in a Remote and Rural Area of Khulna, Bangladesh. *International Scholarly Research Notices*. doi:https://doi.org/10.1155/2014/751952

Brouwer, C., & Heibloem, M. (1986). Irrigation Water Management and Irrigation Water Needs. *FAO - Training manual, 3.*

Brouwer, C., Prins, K., & Heibloem, M. (1989). *Irrigation water management: irrigation scheduling.* Récupéré sur Fao.org: http://www.fao.org/3/T7202E/t7202e00.htm#Contents

Büyükalaca, O., Bulut, H., & Yılmaz, T. (2001). Analysis of variable-base heating and cooling degree-days for Turkey. *Applied Energy, 69(4)*, pp. 269-283.

Carnegie Mellon University (CMU). (s.d.). *Integrated Environmental Control Model.* Récupéré sur Department of Engineering & Public Policy (EPP): https://www.cmu.edu/epp/iecm/

Chinowsky, P. S., Price, J. C., & Neumann, J. E. (2013). Assessment of climate change adaptation costs for the US road network. *Global Environmental Change, 23(4)*, 764-773.

Chinowsky, P., Hayles, C., Schweikert, A., Strzepek, N., Strzepek, K., & Schlosser, A. (2011). Climate change: comparative impact on developing and developed countries. *The Engineering Project Organization Journal*, pp. 67-80.

Choi, T., Keith, L., Hocking, E., Friedman, K., & Matheu, E. (2011). *Dams and energy sectors interdependency study.*

City of Chicago Department of Environment. (2006). *Green roof test plot project: annual project summary report.* Chicago.

Colman, J. (2013, Avril 26). The effect of ambient air and water temperature on power plant efficiency. *Master Thesis*. Duke University Libraries.

Cronshey, R., McCuen, R. H., Miller, N., Rawls, W., Robbins, S., & Woodward, D. (1986, June). *Urban Hydrology for Small Watersheds.* Récupéré sur USDA-United States Department of Agriculture: https://www.nrcs.usda.gov/Internet/FSE_DOCUMENTS/stelprdb1044171.pdf

Das, T. K., Saharawat, Y. S., Bhattacharyya, R., Sudhishri, S., Bandyopadhyay, K. K., Sharma, A. R., & Jat, M. L. (2018). Conservation agriculture effects on crop and water productivity, profitability and soil organic carbon accumulation under a maize-wheat cropping system in the North-western Indo-Gangetic Plains. *Field Crops Research, 215*, pp. 222-231.

Davies, Z. G., Edmondson, J. L., Heinemeyer, A., Leake, J. R., & Gaston, K. J. (2011). Mapping an urban ecosystem service: quantifying above-ground carbon storage at a city-wide scale. *Journal of applied ecology, 48(5)*, pp. 1125-1134.

Davy, R., Gnatiuk, N., Pettersson, L., & Bobylev, L. (2018). Climate change impacts on wind energy potential in the European domain with a focus on the Black Sea. *Renewable and sustainable energy reviews*, pp. 1652-1659.

De Oliveira, V., De Mello, C., Viola, M., & Srinivasan, R. (2017). Assessment of climate change impacts on the streamflow and hydropower potential in the headwater region of the

Grande river basin, Southeastern Brazil. *International Journal of Climatology 37[15]*, pp. 5005-5023.

De Rosa, M., Bianco, V., Scarpa, F., & Tagliafico, L. A. (2014). Heating and cooling building energy demand evaluation; a simplified model and a modified degree days approach. *Applied Energy, 128*, 217-229.

De Sa, A., & Al Zubaidy, S. (2011). Gas turbine performance at varying ambient temperature. *Applied Thermal Engineering, 31(14-15)*, 2735-2739.

Demuzere, M., Orru, K., Heidrich, O., Olazabal, E., Geneletti, D., Orru, H., . . . Faehnle, M. (2014). Mitigating and adapting to climate change: Multi-functional and multi-scale assessment of green urban infrastructure. *Journal of environmental management, 146*, pp. 107-115.

Dhakal, S., & Hanaki, K. (2002). Improvement of urban thermal environment by managing heat discharge sources and surface modification in Tokyo. *Energy and buildings, 34(1)*, pp. 13-23.

Diaz, C. A., Osmond, P., & King, S. (2015). Precipitation and buildings: estimation of the natural potential of locations to sustain indirect evaporative cooling strategies through hot seasons. *Living and Learning: Research for a Better Built Environment: 49th International Conference of the Architectural Science Association*, (pp. 45-54). Melbourne.

Djaman, K., O'Neill, M., Owen, C. K., Smeal, D., Koudahe, K., West, M., & Irmak, S. (2018). Crop evapotranspiration, irrigation water requirement and water productivity of maize from meteorological data under semiarid climate. *MDPI - Water 2018, 10(4), 405*.

Doorenbos, J., & Kassam, A. (1979). *Yield response to Water Irrigation and Drainage.* Roma: Food and Agricultural Organization; Paper No 33.

Drax. (2017, August 29). *Technology - What hot weather means for electricity*. Récupéré sur Drax.com: https://www.drax.com/technology/hot-weather-means-electricity/

Du, L., Trinh, X., Chen, Q., Wang, C., Wang, H., Xia, X., . . . Wu, Z. (2018). Enhancement of microbial nitrogen removal pathway by vegetation in Integrated Vertical-Flow Constructed Wetlands (IVCWs) for treating reclaimed water. *Bioresource technology, 2*.

Dunn, A. D. (2007). *Green light for green infrastructure.* Récupéré sur Digitalcommons.pace.edu: https://digitalcommons.pace.edu/lawfaculty/494

Durmayaz, A., & Sogut, O. S. (2006). Influence of cooling water temperature on the efficiency of a pressurized-water reactor nuclear-power plant. *International Journal of Energy Research, 30(10)*, pp. 799-810.

East Coast Lightning Equipment INC. (s.d.). *Lightning protection installation cost study* . Récupéré sur East Coast Lightning Equipment INC: https://ecle.biz/coststudy/

Eliasson, J., & Ludvigsson, G. (2000). Load factor of hydropower plants and its importance in planning and design. *11th International Seminar on Hydro Power Plants.* Vienna.

El-Refaie, G. (2010). Temperature impact on operation and performance of Lake. *Ain Shams Engineering Journal 1*, 1-9.

El-Shobokshy, M. S., & Hussein, F. M. (1993). Degradation of photovoltaic cell performance due to dust deposition on to its surface. *Renewable Energy, 3(6-7)*, pp. 585-590.

Engineering ToolBox. (2009). *Pumping Water - Energy Cost Calculator*. Récupéré sur engineeringtoolbox.com: https://www.engineeringtoolbox.com/water-pumping-costs-d_1527.html

Engineering ToolBox. (s.d.). *Hydropower*. Récupéré sur Engineering ToolBox: https://www.engineeringtoolbox.com/hydropower-d_1359.html

EPA. (2014). *The Economic Benefits of Green Infrastructure - A Case Study of Lancaster, PA.*

Eurostat. (2019). *Energy statistics - cooling and heating degree days (nrg_chdd)*. Récupéré sur Eurostat, the Statistical Office of the European Union: https://ec.europa.eu/eurostat/cache/metadata/en/nrg_chdd_esms.htm

Eurostat, the Statistical Office of the European Union. (2019). *Energy statistics - cooling and heating degree days (nrg_chdd)*. Récupéré sur Europa.eu: https://ec.europa.eu/eurostat/cache/metadata/en/nrg_chdd_esms.htm

Evans, D. V., & Antonio, F. D. (1986). Hydrodynamics of Ocean Wave-Energy Utilization: IUTAM Symposium Lisbon/Portugal 1985. *Springer Science & Business Media*, pp. 133-156.

Farkas, Z. (2011). *Considering air density in wind power production.* Budapest.

Fisher, J. C., Bartolino, J. R., Wylie, A. H., Sukow, J., & McVay, M. (2016). *Groundwater-flow model for the Wood River Valley aquifer system, south-central Idaho.* US Geological Survey.

Flowers, M. E., Smith, M. K., Parsekian, A. W., Boyuk, D. S., McGrath, J. K., & Yates, L. (2016). Climate impacts on the cost of solar energy. *Energy Policy, 94*, pp. 264-273.

Gajbhiye, S., Mishra, S. K., & Pandey, A. (2013). Effects of Seasonal/Monthly Variation on Runoff Curve Number for Selected Watersheds of Narmada Basin. *International Journal of Environmental Sciences, Volume 3, No 6*, pp. 2019-2030.

Garfí, M., Pedescoll, A., Bécares, E., Hijosa-Valsero, M., Sidrach-Cardona, R., & García, J. (2012). Effect of climatic conditions, season and wastewater quality on contaminant removal efficiency of two experimental constructed wetlands in different regions of Spain. *Science of the total environment, 437*, pp. 61-67.

Georgi, N. J., & Zafiriadis, K. (2006). The impact of park trees on microclimate in urban areas. *Urban Ecosystems, 9(3)*, pp. 195-209.

Ghamami, M., Fayazi Barjin, A., & Behbahani, S. (2016). Performance Optimization of a Gas Turbine Power Plant Based on Energy and Exergy Analysis. *Mechanics, Materials Science & Engineering Journal, 29*.

GIZ. (2016). *Solar Powered Irrigation Systems (SPIS) – Technology, Economy, Impacts.* Récupéré sur Gesellschaft für Internationale Zusammenarbeit (GIZ): https://energypedia.info/images/temp/2/23/20160630122544!phpeKHVUr.pdf

Gomes, J., Diwan, L., Bernardo, R., & Karlsson, B. (2014). Minimizing the Impact of Shading at Oblique Solar Angles in a Fully Enclosed Asymmetric Concentrating PVT Collector. *Energy Procedia (57)*, pp. 2176-2185.

Good, E., & Calaf, S. (2019). Solar PV Power Potential is Greatest Over Croplands. *SciRep (9, 11442)*.

Green, A. (2020). *The intersection of energy and machine learning*. Récupéré sur adgefficiency.com: https://adgefficiency.com/energy-basics-ambient-temperature-impact-on-gas-turbine-performance/

Haerter, J., Hagemann, S., Moseley, C., & Piani, C. (2011). Climate model bias correction and the role of timescales. *Hydrology and Earth System Sciences, 15*, pp. 1065-1073.

Handayani, K., Filatova, T., & Krozer, Y. (2019). The Vulnerability of the Power Sector to Climate Variability and Change: Evidence from Indonesia. *Energies, 12(19), 3640*.

Harrison, G. P., & Whittington, H. W. (2002). Vulnerability of hydropower projects to climate change. *IEE proceedings-generation, transmission and distribution, 149(3)*, pp. 249-255.

Harrison, G., & Wallace, A. (2005). Climate sensitivity of marine energy. *Renewable Energy, 30(12)*, pp. 1801-1817.

Henry, C. L., & Pratson, L. F. (2016). Effects of environmental temperature change on the efficiency of coal-and natural gas-fired power plants. *Environmental science & technology, 50(17)*, 9764-9772.

Hutyra, L. R., Yoon, B., & Alberti, M. (2011). Terrestrial carbon stocks across a gradient of urbanization: a study of the Seattle, WA region. *Global Change Biology, 17(2)*, pp. 783-797.

Ibrahim, S., Ibrahim, M., & Attia, S. (2014). The impact of climate changes on the thermal performance of a proposed pressurized water reactor: nuclear-power plant. *International Journal of Nuclear Energy*.

Jabboury, B. G., & Darwish, M. A. (1990). Performance of gas turbine co-generation power desalting plants under varying operating conditions in Kuwait. *Heat Recovery Systems and CHP, 10(3)*, 243-253.

Jackson, N., & Puccinelli, J. (2006). *Long-Term Pavement Performance (LTPP) data analysis support: National pooled fund study TPF-5 (013)-effects of multiple freeze cycles and deep frost penetration on pavement performance and cost (No. FHWA-HRT-06-121).*

Janssen, H., Carmeliet, J., & Hens, H. (2004). The influence of soil moisture transfer on building heat loss via the ground. *Building and Environment, 39(7)*, 825-836.

Jerez, S., Tobin, I., Vautard, R., Montávez, J. P., López-Romero, J. M., Thais, F., . . . Wild, M. (2015). The impact of climate change on photovoltaic power generation in Europe. *Nature Communications, 6(1)*, pp. 1-8.

Ji, M., Hu, Z., Hou, C., Liu, H., Ngo, H. H., Guo, W., . . . Zhang, J. (2020). New insights for enhancing the performance of constructed wetlands at low temperatures. *Bioresource Technology, 122722*.

JICA. (March 2003). *Manual on flood control planning.* Department of public works and highways.

Jim, C. Y., & Chen, W. Y. (2008). Assessing the ecosystem service of air pollutant removal by urban trees in Guangzhou (China). *Journal of environmental management, 88(4)*, pp. 665-676.

Kadlec, R. H., & Reddy, K. R. (2001). Temperature effects in treatment wetlands. *Water environment research, 73(5)*, pp. 543-557.

Kakaras, E., Doukelis, A., Prelipceanu, A., & Karellas, S. (2006). Inlet air cooling methods for gas turbine based power plants.

Kaldellis, J., & Fragos, P. (2011). Ash deposition impact on the energy performance of photovoltaic generators. *Journal of cleaner production, 19(4)*, pp. 311-317.

Kappos, L., Ntouros, I., & Palivos, I. (1996). Pollution effect on PV system efficiency. *Proceedings of the 5th National Conference on Soft Energy Forms.* Athens.

Kivi, R. (2017, Avril 24). *How Does Geothermal Energy Work?* Récupéré sur Sciencing: https://sciencing.com/geothermal-energy-work-4564716.html

Kloss, C., & Calarusse, C. (2011). *Rooftops to Rivers: Green strategies for controlling stormwater and combined sewer overflows.* New-York.

Koc, C. B., Osmond, P., & Peters, A. (2018). Evaluating the cooling effects of green infrastructure: A systematic review of methods, indicators and data sources. *Solar Energy, 166*, pp. 486-508.

Koch, H., & Vögele, S. (2009). Dynamic modelling of water demand, water availability and adaptation strategies for power plants to global change. *Ecological Economics, 68(7)*, pp. 2031-2039.

Kosa, P. (2011). The effect of temperature on actual evapotranspiration based on Landsat 5 TM Satellite Imagery. *Evapotranspiration, 56(56)*, pp. 209-228.

Krishna, P., Kumar, K., & Bhandari, N. M. (2002). IS: 875 (Part3): Wind loads on buildings and structures-proposed draft & commentary. Document No.: IITK-GSDMA-Wind, 02-V5. Roorkee, Uttarakhand, India: Department of Civil Engineering; Indian Institute of Technology Roorkee.

Kumpulainen, L., Laaksonen, H., Komulainen, R., Martikainen, A., Lehtonen, M., Heine, P., . . . Saaristo, H. (2007). *Distribution Network 2030 - Vision of the future power system.* Finland: VTT.

Land, M., Granéli, W., Grimvall, A., Hoffmann, C. C., Mitsch, W. J., Tonderski, K. S., & Verhoeven, J. T. (2016). How effective are created or restored freshwater wetlands for nitrogen and phosphorus removal? A systematic review. *Environmental Evidence, 5*.

Larsen, P., Goldsmith, S., Wilson, M., Strzepek, K., Chinowsky, P., & Saylor, B. (2008). Estimating future costs for Alaska public infrastructure at risk from climate. *Global Environmental Change*, pp. 442-457.

Lavin, P. (2003). *A Practical Guide to Design, Production, and Maintenance for Architects and Engineers.* London/New-York: Spon Press.

Law, Y., Ye, L., Pan, Y., & Yuan, Z. (2012). Nitrous oxide emissions from wastewater treatment processes. *Philosophical Transactions of the Royal Society B: Biological Sciences, 367(1593)*, pp. 1265-1277.

Linnerud, K., Mideksa, T. K., & Eskeland, G. S. (2011). The impact of climate change on nuclear power supply. *The Energy Journal, 32(1)*.

Lise, W., & van der Laan, J. (2015). Investment needs for climate change adaptation measures of electricity power plants in the EU. *Energy for Sustainable Development, 28*, pp. 10-20.

Mamo, G. E., Marence, M., Hurtado, J. C., & Franca, M. J. (2018). Optimization of Run-of-River Hydropower Plant Capacity.

Manoli, G., Fatichi, S., Schläpfer, M., Yu, K., Crowther, T. W., Meili, N., . . . Bou-Zeid, E. (2019). Magnitude of urban heat islands largely explained by climate and population. *Manoli, G., Fatichi, S., Schläpfer, M., Yu, K., Crowther, T. W., Meili, N., ... & Bou-Zeid, E. (2019). Magnitude of urban Nature, 573(7772)*, pp. 55-60.

Manwell, J. F., McGowan, J. G., & Rogers, A. L. (2010). *Wind energy explained: theory, design and application.* John Wiley & Sons.

Manwell, J., McGowan, J., & Rogers, A. (2002). *Wind Energy Explained: Theory, Design and Application.*

Maulbetsch, J. S., & Di Filippo, M. N. (2006). *Cost and value of water use at combined-cycle power plants.* California: California Energy Commission - Public Interest Energy Research Program.

Maupoux, M. (2010). *Solar photovoltaic water pumping.* Récupéré sur Practical Action - The Schumacher Centre for Technology and Development : https://sswm.info/sites/default/files/reference_attachments/MAUPOUX%202010%20Solar%20Water%20Pumping.pdf

Meral, M. E., & Dincer, F. (2011). A review of the factors affecting operation and efficiency of photovoltaic based electricity generation systems. *Renewable and Sustainable Energy Reviews, 15(5)*, pp. 2176-2184.

Mimikou, M. A., & Baltas, E. A. (1997). Climate change impacts on the reliability of hydroelectric energy production. *Hydrological Sciences Journal, 42(5)*, pp. 661-678.

Miradi, M. (2004). Artificial neural network (ANN) models for prediction and analysis of ravelling severity and material composition properties. *CIMCA*, pp. 892-903.

Mirgol, B., Nazari, M., & Eteghadipour, M. (2020). Modelling Climate Change Impact on Irrigation Water Requirement and Yield of Winter Wheat (Triticum aestivum L.), Barley (Hordeum vulgare L.), and Fodder Maize (Zea mays L.) in the Semi-Arid Qazvin Plateau, Iran. *Agriculture, 10(3), 60*.

Mourshed, M. (2012). Relationship between annual mean temperature and degree-days. *Energy and buildings, 54*, pp. 418-425.

N.D. Lea International. (1995). *Modelling Road Deterioration and Maintenance.* Prepared for the Asian Development Bank.

N.D. Lea International. (1995). *Modelling Road Deterioration and Maintenance.* Prepared for the Asian Development Bank.

National Snow & Ice Data Center. (n.d.). *freezing degree-days*. Retrieved from https://nsidc.org/cryosphere/glossary/term/freezing-degree-days

Nazahiyah, R., Yusop, Z., & Abustan, I. (2007). Stormwater quality and pollution loading from an urban residential catchment in Johor, Malaysia. *Water science and technology, 56(7)*, pp. 1-9.

Nemry, F., & Demirel, H. (2012). *Impacts of Climate Change on Transport: A focus on road and rail transport infrastructures.* Luxembourg: Publications Office of the European Union.

Nichol, J. E. (1996). High-resolution surface temperature patterns related to urban morphology in a tropical city: A satellite-based study. *Journal of applied meteorology, 35(1)*, pp. 135-146.

Nordhaus, W. (2017). Revisiting the social cost of carbon. *PNAS*, vol. 11, no.7, 1518-1523.

Nowak, D. J., Greenfield, E. J., Hoehn, R. E., & Lapoint, E. (2013). Carbon storage and sequestration by trees in urban and community areas of the United States. *Environmental pollution, 178, 229-236.*, pp. 229-236.

Ould-Amrouche, S., Rekioua, D., & Hamidat, A. (2010). Modelling photovoltaic water pumping systems and evaluation of their CO2 emissions mitigation potential. *Applied Energy, 87*, pp. 3451-3459.

Panagea, I. S., Tsanis, I. K., Koutroulis, A. G., & Grillakis, M. G. (2014). Climate change impact on photovoltaic energy output: the case of Greece. *Advances in Meteorology*.

Pande, P., & Telang, S. (2014). Calculation of Rainwater Harvesting Potential by Using Mean Annual Rainfall, Surface Runoff and Catchment Area. *Green Clean Guide, India, Global Advanced Research Journal of Agricultural Science, Vol 3(7)*, 200-204.

Parker, J. H. (1989, February). The impact of vegetation on air conditioning consumption. *In Proceedings of the Workshop on Saving Energy and Reducing Atmospheric Pollution by Controlling Summer Heat Islands (pp. 45-52).*

Parliamentary Office of Science and Technology (POST). (2011). *Carbon footprint of electricity generation.* Récupéré sur POST Note Update, 383:

https://www.parliament.uk/documents/post/postpn_383-carbon-footprint-electricity-generation.pdf

Pérez, G., Coma, J., Martorell, I., & Cabeza, L. F. (2014). Vertical Greenery Systems (VGS) for energy saving in buildings: A review. *Renewable and Sustainable Energy Reviews, 39*, pp. 139-165.

Petchers, N. (2003). *Combined heating, cooling & power handbook: technologies & applications: an integrated approach to energy resource optimization.* Fairmont Press.

Photovoltaic Softwares. (2020). *Photovoltaic Softwares*. Récupéré sur photovoltaic-software.com: https://photovoltaic-software.com/principle-ressources/how-calculate-solar-energy-power-pv-systems

Pierson Jr, W., & Moskowitz, L. (1964). A proposed spectral form for fully developed wind seas based on the similarity theory of SA Kitaigorodskii. *Journal of geophysical research*, pp. 5181-5190.

Plósz, B. G., Liltved, H., & Ratnaweera, H. (2009). Climate change impacts on activated sludge wastewater treatment: a case study from Norway. *Water Science and Technology, 60(2)*, pp. 533-541.

Poullain, J. (2012). *PDHonline Course H119 (2 PDH) - Estimating Storm Water Runoff.* Récupéré sur pdhonline.org: https://pdhonline.com/courses/h119/stormwater%20runoff.pdf

Prado, R. T., & Ferreira, F. L. (2005). Measurement of albedo and analysis of its influence the surface temperature of building roof materials. *Energy and Buildings, 37(4)*, 295-300.

Rademaekers, K., van der Laan, J., Boeve, S., Lise, W., van Hienen, J., Metz, B., . . . Kirchsteiger, C. (2011). *Investment needs for future adaptation measures in EU nuclear power plants and other electricity generation technologies due to effects of climate change .* Brussels: Library (DM28, 0/36).

Ramos-Scharron, C., & MacDonald, L. (2007). Runoff and suspended sediment yields from an unpaved road segment. *Hydrological Processes, 21(1)*, pp. 35-50.

Rodell, M., Chen, J., Kato, H., Famiglietti, J. S., Nigro, J., & Wilson, C. R. (2007). Estimating groundwater storage changes in the Mississippi River basin (USA) using GRACE. *Hydrogeology Journal 15[1]*, pp. 159-166.

Roorda, J., & van der Graaf, J. (2000). Understanding membrane fouling in ultrafiltration of WWTP-effluent. *Water Science and Technology 41(10-11)*, pp. 345-353.

Rousseau, Y. (2013). Impact of Climate Change on Thermal Power Plants. Case study of thermal power plants in France.

Sahely, H. R., MacLean, H. L., Monteith, H. D., & Bagley, D. M. (2006). Comparison of on-site and upstream greenhouse gas emissions from Canadian municipal wastewater treatment facilities. *Journal of Environmental Engineering and Science, 5(5)*, pp. 405-415.

Saito, I., Ishihara, O., & Katayama, T. (1990). Study of the effect of green areas on the thermal environment in an urban area. *Energy and buildings, 15(3-4)*, pp. 493-498.

Santamouris, M. (2014). Cooling the cities–a review of reflective and green roof mitigation technologies to fight heat island and improve comfort in urban environments. *Solar energy, 103*, pp. 682-703.

Scheehle, E. A., & Doorn, M. R. (2012). *Estimate of United States GHG Emissions from wastewater.* Récupéré sur EPA.org: https://www3.epa.gov/ttn/chief/conference/ei12/green/present/scheele.pdf

Scheehle, E. A., & Doorn, M. R. (2012). *Improvements to the U.S. Wastewater Methane and Nitrous Oxide Emissions.* Récupéré sur EPA.org: https://www3.epa.gov/ttn/chief/conference/ei12/green/scheehle.pdf

Schnetzer, J., & Pluschke, L. (2017). *Solar-Powered Irrigation Systems: A clean-energy, low-emission option for irrigation development and modernization.* FAO.

Shukla, A. K., & Singh, O. (2014). Effect of Compressor Inlet Temperature & Relative Humidity on Gas Turbine Cycle Performance. *International Journal of Scientific & Engineering Research, 5(5)*, 664-670.

Shukla, A. K., & Singh, O. (2014). Effect of Compressor Inlet Temperature & Relative Humidity on Gas Turbine Cycle Performance. *International Journal of Scientific & Engineering Research, 5(5)*, 664-670.

Singh, S., & Kumar, R. (2012). Ambient air temperature effect on power plant performance. *International Journal of Engineering Science and Technology*.

Singh, S., & Tiwari, S. (2019). *Climate Change, Water and Wastewater Treatment: Interrelationship and Consequences.* Singapore: Springer.

Song, Z., Zheng, Z., Li, J., Sun, X., Han, X., Wang, W., & Xu, M. (2006). Seasonal and annual performance of a full-scale constructed wetland system for sewage treatment in China. *Ecological Engineering, 26(3)*, pp. 272-282.

Souch, C. A., & Souch, C. (1993). The effect of trees on summertime below canopy urban climates: a case study Bloomington. *Journal of Arboriculture, 19(5)*, pp. 303-312.

Taha, H. (1996). Modeling impacts of increased urban vegetation on ozone air quality in the South Coast Air Basin. *Atmospheric Environment, 30(20)*, pp. 3423-3430.

Taha, H. (1997). Urban climates and heat islands; albedo, evapotranspiration, and anthropogenic heat. *Energy and buildings, 25(2).*

Taha, H., Akbari, H., & Rosenfeld, A. (1988). Vegetation Canopy Micro-Climate: A Field-Project in Davis, California. *Journal of Climate and Applied Meteorology*.

Taha, H., Akbari, H., & Rosenfeld, A. (1991). Heat island and oasis effects of vegetative canopies: micro-meteorological field-measurements. *Theoretical and Applied Climatology, 44(2)*, pp. 123-138.

Tallis, M., Taylor, G., Sinnett, D., & Freer-Smith, P. (2011). Estimating the removal of atmospheric particulate pollution by the urban tree canopy of London, under current and future environments. *Landscape and Urban Planning, 103(2)*, pp. 129-138.

Tang, H. (2012). Research on Temperature and Salt Migration Law of Sulphate Salty Soil Subgrade in Xinjiang Region. Beijing, China: Beijing Jiaotong University.

Taylor, C. R., Hook, P. B., Stein, O. R., & Zabinski, C. A. (2011). Seasonal effects of 19 plant species on COD removal in subsurface treatment wetland microcosms. *Ecological Engineering, 37(5)*, pp. 703-710.

Tiwary, A., Sinnett, D., Peachey, C., Chalabi, Z., Vardoulakis, S., Fletcher, T., . . . Hutchings, T. R. (2009). An integrated tool to assess the role of new planting in PM10 capture and the human health benefits: A case study in London. *Environmental pollution, 157(10)*, pp. 2645-2653.

Tran, Q. K., Jassby, D., & Schwabe, K. A. (2017). The implications of drought and water conservation on the reuse of municipal wastewater: Recognizing impacts and identifying mitigation possibilities. *Water research, 124*, 472-481.

Tsihrintzis, V. A., & Hamid, R. (1998). Runoff quality prediction from small urban catchments using SWMM. *Hydrological Processes, 12(2)*, pp. 311-329.

U.S. DoE. (2013). *U.S. Energy sector vulnerabilities to climate change and extreme weather.* DOE/PI-0013: U.S. Department of Energy.

U.S. Environmental Protection Agency. (2003, September). *Cooling summertime temperatures: Strategies to reduce heat islands.* Récupéré sur epa.gov: https://www.epa.gov/sites/production/files/2014-06/documents/hiribrochure.pdf

Ullrich, A., & Volk, M. (2009). Application of the Soil and Water Assessment Tool (SWAT) to predict the impact of alternative management practices on water quality and quantity. *Agricultural Water Management, 96(8)*, pp. 1207-1217.

UNEP. (2015). *Economic Valuation of Wastewater - The Cost of Action and the Cost of No Action.* United Nations Environment Programme (UNEP), commissioned by the Global Programme of Action for the Protection of the Marine Environment from Land-based Activities (GPA), through the Global Wastewater Initiative (GW2I).

URS Corporation Limited. (2010). *Adapting Energy, Transport and Water Infrastructure to the Long-term Impacts of Climate Change .* San Francisco, CA, USA, Report RMP/5456.

Valkama, P., Mäkinen, E., Ojala, A., Vahtera, H., Lahti, K., Rantakokko, K., . . . Wahlroos, O. (2017). Seasonal variation in nutrient removal efficiency of a boreal wetland detected by high-frequency on-line monitoring. *Ecological engineering, 98*, pp. 307-317.

Van Vliet, M. T., Yearsley, J. R., Ludwig, F., Vögele, S., Lettenmaier, D. P., & Kabat, P. (2012). Vulnerability of US and European electricity supply to climate change. *Nature Climate Change, 2(9)*, 676-681.

Vought, T. D. (2019, June 30). *An Economic Case for Facility Lightning Protection Systems in 2017*. Récupéré sur VFC: https://vfclp.com/articles/an-economic-case-for-facility-lightning-protection-systems-in-2017/

Watkins, R., Littlefair, P., Kolokotroni, M., & Palmer, J. (2002). The London heat island–Surface and air temperature measurements in a park and street gorges. *ASHRAE Transactions, 108(1)*, pp. 419-427.

Wilbanks, T., Bhatt, V., Bilello, D., Bull, S., Ekmann, J., Horak, W., & Huang, Y. J. (2008). *Effects of Climate Change on Energy Production and Use in the United States.* Lincoln: US Department of Energy Publications.

Xiao, Q., & McPherson, E. G. (2002). Rainfall interception by Santa Monica's municipal urban forest. *Urban ecosystems, 6(4)*, pp. 291-302.

Yamba, F., Walimwipi, H., Jain, S., Zhou, P., Cuamba, B., & Mzezewa, C. (2011). Climate change/variability implications on hydroelectricity generation in the Zambezi River Basin. *Mitigation and Adaptation Strategies for Global Change*, pp. 617-628.

Young, I. R., & Holland, G. J. (1996). Atlas of the oceans: wind and wave climate. *Oceanographic Literature Review, 7(43), 742*.

Yuan, H., Nie, J., Zhu, N., Miao, C., & Lu, N. (2013). Effect of temperature on the wastewater treatment of a novel anti-clogging soil infiltration system. *Ecological engineering, 57*, pp. 375-379.

Zhang, C., Liao, H., & Mi, Z. (2019). Climate impacts: temperature and electricity consumption. *Natural Hazards, 99(3)*, pp. 1259-1275.

Zhang, Y., Kendy, E., Qiang, Y., Changming, L., Yanjun, S., & Hongyong, S. (2004). Effect of soil water deficit on evapotranspiration, crop yield, and water use efficiency in the North China Plain. *Agricultural Water Management, 64*(2), pp. 107-122.

Zhao, C., Liu, B., Piao, S., Wang, X., Lobell, D., Huang, Y., ... (2017). Temperature increase reduces global yields of major crops in four independent estimates. *Proceedings of the National Academy of Sciences, 114 (35)*. doi:https://doi.org/10.1073/pnas.1701762114

Zhao, M., Kong, Z. H., Escobedo, F. J., & Gao, J. (2010). Impacts of urban forests on offsetting carbon emissions from industrial energy use in Hangzhou, China. *Journal of Environmental Management, 91(4)*, pp. 807-813.

Zhao, X., Shen, A., & Ma, B. (2018). Temperature Adaptability of Asphalt Pavement to High Temperatures and Significant Temperature Differences. *Advances in Materials Science and Engineering*.

Zheng, S., Huang, G., Zhou, X., & Zhu, X. (2020). Climate-change impacts on electricity demands at a metropolitan scale: A case study of Guangzhou, China. *Applied Energy, 261, 114295*.

Zhou, Z. C., Shangguan, Z. P., & Zhao, D. (2006). Modeling vegetation coverage and soil erosion in the Loess Plateau Area of China. *Ecological modelling, 198(1-2)*, pp. 263-268.

Zoppou, C. (2001). Review of urban storm water models. *Environmental Modelling & Software, 16(3)*, pp. 195-231.

Zouboulis, A., & Tolkou, A. (2016). Effect of climate change in wastewater treatment plants: reviewing the problems and solutions. Dans S. A. Shrestha, *Managing Water Resources under Climate Uncertainty* (pp. 197-220). Springer.

Zoulia, I., Santamouris, M., & Dimoudi, A. (2009). Monitoring the effect of urban green areas on the heat island in Athens. *Environmental monitoring and assessment, 156(1-4)*.

Zsirai, T., Buzatu, P., Maffettone, R., & Judd, S. (2012, April). *Sludge viscosity—The thick of it*. Récupéré sur The MBR (Membrane Bioreactors): https://www.thembrsite.com/features/sludge-viscosity-in-membrane-bioreactors-the-thick-of-it/

Annex I: Code for establishing the CDS Toolbox-SAVi link

Code related to offline processing of CDS Toolbox and CDS API data for the C3S_428h_IISD-EU project.

How does this code relate to the CDS API ?

This code builds on the powerful CDS API but focuses on local impact analysis specific for the C3S_428h_IISD-EU project. It makes it easier to retrieve a time series for a specific location or region, and save the result to a CSV file (a simpler format than netCDF for most climate adaptation practitioners). Additionally, the code combines variables across multiple datasets, aggregate them into asset classes (such as all energy-related variables) and perform actions such as bias correction (use of ERA5 and CMIP5).

Code available for download

The easy way is to download the zipped archive: - latest (development): https://github.com/perrette/iisd-cdstoolbox/archive/master.zip - or check stable releases with description of changes: https://github.com/perrette/iisd-cdstoolbox/releases (see assets at the bottom of each release to download a zip version)

The hacky way is to use git (only useful during development, for frequent updates, to avoid having to download and extract the archive every time):

- First time: `git clone https://github.com/perrette/iisd-cdstoolbox.git`

- Subsequent updates: `git pull` from inside the repository

Installation steps

- Download the code (see above) and inside the folder.
- Install Python 3, ideally Anaconda Python which comes with pre-installed packages
- Install the CDS API key: https://cds.climate.copernicus.eu/api-how-to
- Install the CDS API client: pip install cdsapi
- Install other dependencies: conda install --file requirements.txt or pip install -r requirements.txt
- *Optional* dependency for coastlines on plots: conda install -c conda-forge cartopy or see docs
- *Optional* dependency: CDO (might be needed later, experimental): conda install -c conda-forge python-cdo

Troubleshooting: - If install fails, you may need to go through the dependencies in requirements.txt one by one and try either pip install or conda install or other methods specific to that dependency. - In the examples that follow, if you have both python2 and python3 installed, you might need to replace python with python3.

CDS API

Download indicators associated with one asset class.

Examples of use:

```
python download.py --asset energy --location Welkenraedt
```

The corresponding csv time series will be stored in `indicators/welkenraedt/energy`. Note that raw downloaded data from the CDS API (regional tiles in netcdf format, and csv for the required lon/lat, without any correction) are stored under `download/` and can be re-used across multiple indicators.

The `indicators` folder is organized by location, asset class, simulation set and indicator name. The aim is to provide multiple sets for SAVi simulation. For instance, `era5` for past simulations, and various `cmip5` versions for future simulations, that may vary with model and experiment. For instance the above command creates the folder structure (here a subset of all variables is shown):

```
indicators/
  welkenraedt/
    energy/
      era5/
        2m_temperature.csv
        precipitation.csv
        ...
      cmip5-ipsl_cm5a_mr-rcp_8_5/
        2m_temperature.csv
        precipitation.csv
        ...
      ...
```

with two simulation sets `era5` and `cmip5-ipsl_cm5a_mr-rcp_8_5`. It is possible to specify other models and experiment via `--model` and `--experiment` parameters, to add further simulation sets and thus test how the choice of climate models and experiment affect the result of SAVi simulations.

Compared to raw CDS API, some variables are renamed and scaled so that units match and are the same across simulation sets. For instance, temperature was adjusted from Kelvin to degree Celsius, and precipitation was renamed and units-adjusted into mm per month from original (mean_total_precipitation_rate (mm/s) in ERA5, and mean_precipitation_flux (mm/s) in CMIP5). Additionally, CMIP5 data is corrected so that climatological mean matches with ERA5 data (climatology computed over 1979-2019 by default).

Additionally to the files shown in the example folder listing above, figures can also be created for rapid control of the data, either for interactive viewing (`--view-timeseries` and `--view-region`) or or saved as PNG files (`--png-timeseries` and `--png-region`), e.g.

```
python download.py --asset energy --location Welkenraedt --png-timeseries --
png-region
```

Single indicators can be downloaded via:

```
python download.py --indicator 2m_temperature --location Welkenraedt
```

The choices available for `--indicator` , `--asset` and `--location` area defined in the following configuration files, respectively:

- controls which indicators are available, how they are renamed and unit-adjusted: indicators.yml (see sub-section below)
- controls the indicator list in each asset class: assets.yml
- controls the list of locations available: locations.yml

Full documentation, including fine-grained controls, is provided in the command-line help:

```
python download.py --help
```

Visit the CDS Datasets download pages, for more information about available variables, models and scenarios:

- ERA5: https://cds.climate.copernicus.eu/cdsapp#!/dataset/reanalysis-era5-single-levels-monthly-means?tab=form

- CMIP5: https://cds.climate.copernicus.eu/cdsapp#!/dataset/projections-cmip5-monthly-single-levels?tab=form

In particular, clicking on “Show API request” provides information about spelling of the parameters, e.g. that “2m temperature” is spelled `2m_temperature` and “RCP 8.5” is spelled `rcp_8_5`.

Indicator definition

This section is intended for users who wish to extend the list of indicators currently defined in indicators.yml. It can be safely ignored for users who are only interested in using the existing indicators.

Let’s see how `10m_wind_speed` is defined:

```
- name: 10m_wind_speed
  units: m / s
  description: Wind speed magnitude at 10 m
```

The fields `name` and `units` define the indicator. Description is optional, just to provide some context. It is possible to provide `scale` and `offset` fields to correct the data as `(data + offset) * scale`. Here for `2m temperature`:

```
- name: 2m_temperature
  units: degrees Celsius
  description: 2-m air temperature
  offset: -273.15  # Kelvin to degrees C
```

# denotes a comment to provide some context. Some indicators have different names in ERA5 and CMIP5, and possibly different units. That can be dealt with by providing `era5` and `cmip5` fields, which have precedence over the top-level fields. Here the `evaporation` definition:

```
- name: evaporation
  units: mm per month
  era5:
    name: mean_evaporation_rate  # different name in ERA5
    scale: -2592000  # change sign and convert from mm/s to mm / month
  cmip5:
    scale: 2592000  # mm/s to mm / month
```

In that case both scaling and name depend on the dataset. In CMIP5 which variable name is identical to our indicator name, the `name` field can be omitted. In ERA5, evaporation is negative (downwards fluxes are counted positively), whereas it is counted positively in ERA5.

Indicators composed of several CDS variables can be defined via `compose` and `expression` fields. Let's look at `100m_wind_speed`:

```
- name: 100m_wind_speed
  units: m / s
  description: Wind speed magnitude at 100 m
  era5:
    compose:
      - 100m_u_component_of_wind
      - 100m_v_component_of_wind
    expression: (_100m_u_component_of_wind**2 + _100m_v_component_of_wind**2)
**0.5
  cmip5:
    name: 10m_wind_speed
    scale: 1.6  # average scaling from 10m to 100m, based on one test locatio
n (approximate!)
```

In ERA5, vector components of 100m wind speed are provided. Our indicator is therefore a composition of these two variables, defined by the `expression` field, which is evaluated as a python expression. Note that variables that start with a digit are not licit in python and must be prefixed with an underscore _ in the `expression` field (only there).

For complex expressions, it is possible to provide a `mapping` field to store intermediate variables, for readability. This is used for the `relative_humidity` indicator:

```
- name: relative_humidity
  units: '%'
  era5:
    compose:
```

```
      - 2m_temperature
      - 2m_dewpoint_temperature
    expression: 100*(exp((17.625*TD)/(243.04+TD))/exp((17.625*T)/(243.04+T)))
    mapping: {T: _2m_temperature - 273.15, TD: _2m_dewpoint_temperature - 273
.15}
  cmip5:
    name: near_surface_relative_humidity
```

where `T` and `TD` are provided as intermediary variables, to be used in `expression`.

ERA5-hourly dataset can be retrieved via `frequency: hourly` field, and subsequently aggregated to monthly indicators thanks to pre-defined functions `daily_max`, `daily_min`, `daily_mean`, `monthly_mean`, `yearly_mean`. For instance:

```
- name: maximum_daily_temperature
  units: degrees Celsius
  offset: -273.15
  cmip5:
    name: maximum_2m_temperature_in_the_last_24_hours
  era5:
    name: 2m_temperature
    frequency: hourly
    transform:
      - daily_max
      - monthly_mean
```

This variable is available directly for CMIP5, but not in ERA5. It is calculated from `2m_temperature` from ERA5 `hourly` dataset, and subsequently aggregated. Note the ERA5-hourly dataset takes significantly longer to retrieve than ERA5 monthly. Consider using in combination with `--year 2000` to retrieve a single year of the ERA5 dataset.

Currently CMIP5 daily is not supported.

Netcdf to csv conversion

Convert netcdf time series files downloaded from the CDS Toolbox pages into csv files (note: this does not work for netcdf files downloaded via the cds api):

```
python netcdf_to_csv.py data/*nc
```

Help:
```
python netcdf_to_csv.py --help
```

Copernicus Climate Change Service